Measurement of the polarization of the *K*-shell resonance line emission of S^{13+} and S^{14+} at relativistic electron beam energies

D. L. Robbins,[1] A. Ya. Faenov,[2] T. A. Pikuz,[2] H. Chen,[3] P. Beiersdorfer,[3] M. J. May,[3] J. Dunn,[3] K. J. Reed,[3] and A. J. Smith[1]

[1]*Department of Physics, Morehosue College, Atlanta, Georgia 30314, USA*

[2]*Multicharged Ions Spectra Data Center of VNIIFTRI, Mendeleevo, Moscow Region, 141570, Russia*

[3]*Lawrence Livermore National Laboratory, Livermore, California 94550, USA*

(Received 12 April 2004; published 31 August 2004)

We have measured the polarization of the heliumlike sulfur resonance line $1s2p\ ^1P_1 \rightarrow 1s^2\ ^1S_0$ and of the blend of the lithiumlike sulfur resonance lines $1s2s2p\ ^2P_{3/2} \rightarrow 1s^22s\ ^2S_{1/2}$ and $1s2s2p\ ^2P_{1/2} \rightarrow 1s^22s\ ^2S_{1/2}$ as a function of electron beam energy from near threshold to 144 keV. These lines were excited with the LLNL high-energy electron beam ion trap and measured using a newly modified two-crystal technique. Our results test polarization predictions in an energy regime where few empirical results have been reported. We also present calculations of the polarization using two different methods, and good agreement is obtained.

DOI: 10.1103/PhysRevA.70.022715 PACS number(s): 34.80.Kw, 52.27.Ny, 32.30.Rj

I. INTRODUCTION

Previous studies have highlighted the possibility of using polarization of x-ray line emissions as a plasma diagnostic tool to infer the presence of directional electrons [1,2]. This diagnostic has been successfully applied to the study of laser-produced plasmas [3], vacuum spark plasmas [4], and Z-pinches [5,6]. It also has been used to determine the electron cyclotron energy component of the electron beam in an electron beam ion trap [7]. Additional polarization effects on the *K*-shell line emission have been predicted in laser-produced plasmas [8].

Theoretical studies of line polarization have been presented by Reed and Chen [9], Itikawa *et al.* [10], Zhang *et al.* [11], and Inal and Dubau [1]. These predictions have been tested by various measurements. Henderson *et al.* reported the first x-ray emission line polarization measurement of a highly charged ion, heliumlike Sc^{19+} [12]. Other reported polarization measurements include Fe^{23+}, Fe^{24+}, Ba^{46+}, Ti^{19+}, and Ti^{20+}, and Ti^{21+}, [13–18]. Polarization measurements of the *K*-shell x-ray emission lines of heliumlike ions were made at single beam energies near threshold of the corresponding resonance lines. The polarization of the magnetic quadrupole transition in neonlike Ba^{46+} was measured at a number of electron impact energies above but still close to the excitation threshold. None of these measurements were made at relativistic energies. Measurement of the polarization of the Lyman-α_1 line in hydrogenlike Ti^{21+}, was presented recently which extended to electron impact energies of 50 keV (10 threshold units). The results reported in Ref. [18] showed unexplained systematic discrepancy with the theoretical predictions. These results motivate further studies at high collision energies. In this paper we report the measurement of the polarization of both heliumlike and lithiumlike sulfur resonance lines as a function of electron impact energy up to ~60 threshold units. We also present calculations based on two different computer codes in this relativistic energy regime, which agree well with the measurements.

II. EXPERIMENTAL MEASUREMENT

The polarization measurements reported here were made using the Lawrence Livermore National Laboratory SuperEBIT electron beam ion trap [19]. The sulfur ions were electrostatically trapped and probed with a quasi-mono-energetic electron beam ~60 μm in diameter. The electron beam was tuned to energies ranging from 3 to 144 keV for these measurements. Past measurements on the Livermore electron beam ion trap have used the "two-crystal technique" [13,14]. The main idea of this technique is to use two crystal spectrometers: one of them aligned at a Bragg angle near 45° and another one far from such an angle. Both crystal spectrometers employ a spectral dispersion plane perpendicular to the electron beam propagation. In a second approach, only one crystal spectrometer has a dispersion plane in the direction perpendicular to the electron beam propagation. The second spectrometer has a dispersion plane parallel to the electron beam propagation. Because of the extended x-ray source size in the direction parallel to the electron beam propagation (15–20 mm) it is necessary to use a focusing crystal spectrometer, as shown in Fig 1. This arrangement is similar to that used by Henderson *et al.* [12]. However, they only had one spectrometer available, thus their measurements were not taken concurrently.

The second approach described above has been utilized here to infer the polarization of the *K*-shell resonance lines of S^{13+} and S^{14+}. As illustrated in Fig. 1, two polarization sensitive crystal spectrometers which act as polarizers were installed on SuperEBIT for simultaneous spectroscopic measurements. One spectrometer, a flat crystal spectrometer (FCS) [20], was equipped with a PET (002) crystal which has a lattice spacing of $2d = 8.742$ Å, which resulted in a Bragg angle of $\theta_B = 35.2°$ for observing the $K\alpha$ transition of heliumlike sulfur. A position sensitive proportional counter

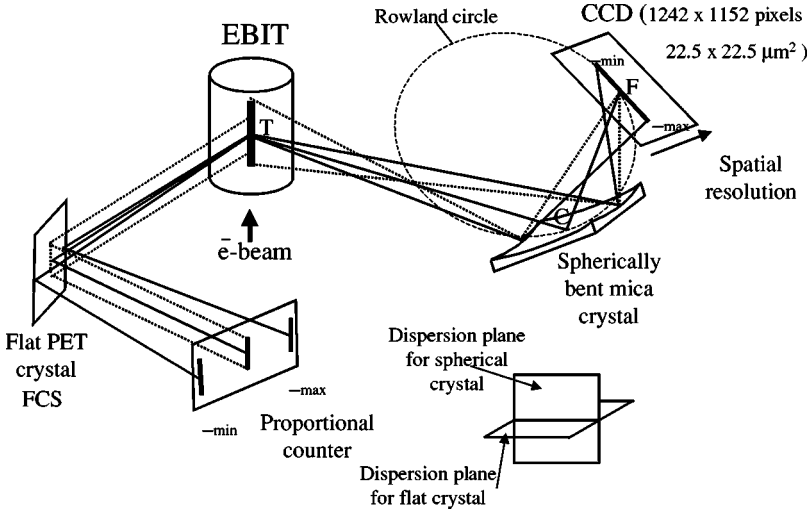

FIG. 1. Electron beam ion trap x-ray polarization measurement setup (modified "two-crystal technique"). FCS preferentially reflects $I_{\parallel}$, while the spherically bent crystal spectrometer reflects $I_{\perp}$.

was used in connection with the FCS for x-ray detection. The second spectrometer (a compact spherical crystal spectrometer [21,22]), employed a Mica (002) crystal bent to a radius of 15 cm. The lattice spacing of $2d=19.942$ Å resulted in a Bragg angle of $\theta_B=49.6°$ for the transition of interest observed in third order reflection. A charged-coupled device (CCD) was used with this spectrometer for x-ray detection. Figures 2–5 show typical spectra obtained by each spectrometer for different electron beam energies. These figures show that FCS produced spectra with a high signal-to-noise ratio, though somewhat lower resolution than the compact focusing spectrometer. The comparatively poor quantum efficiency and high noise level of the CCD detector hampered the latter.

III. ANALYSIS

The intensities observed by the crystal spectrometers can be expressed as

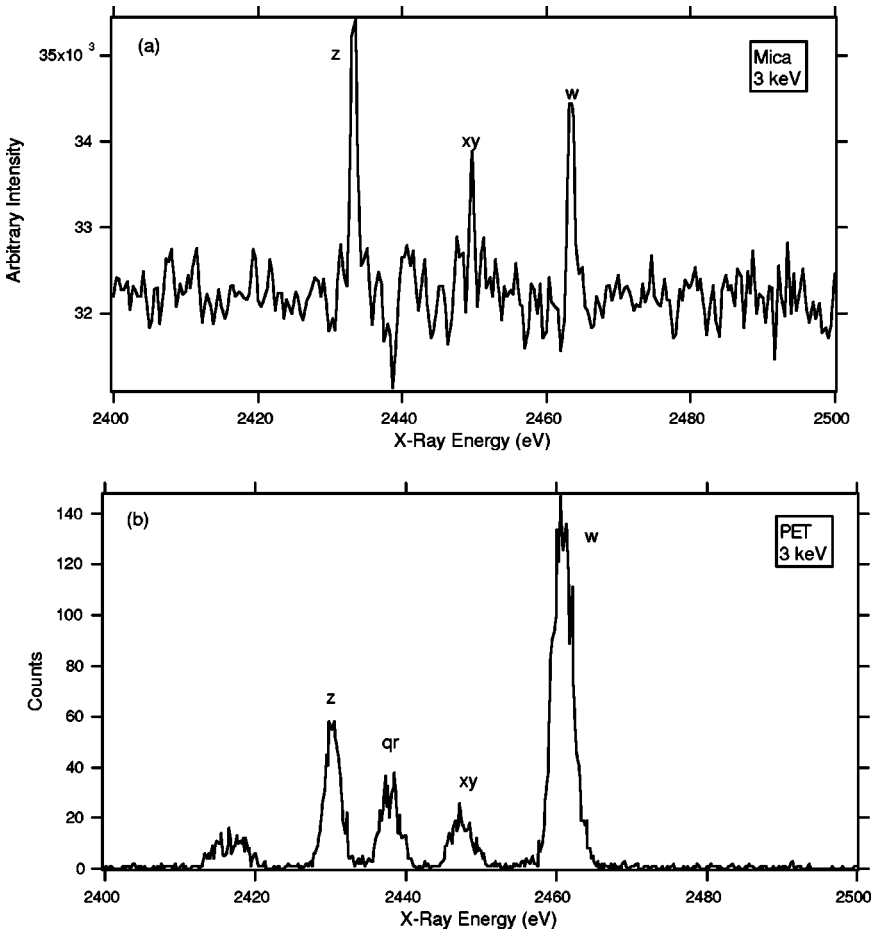

FIG. 2. Spectra obtained with (a) the spherically bent crystal spectrometer and (b) the flat crystal spectrometer (electron beam energy: 3 keV).

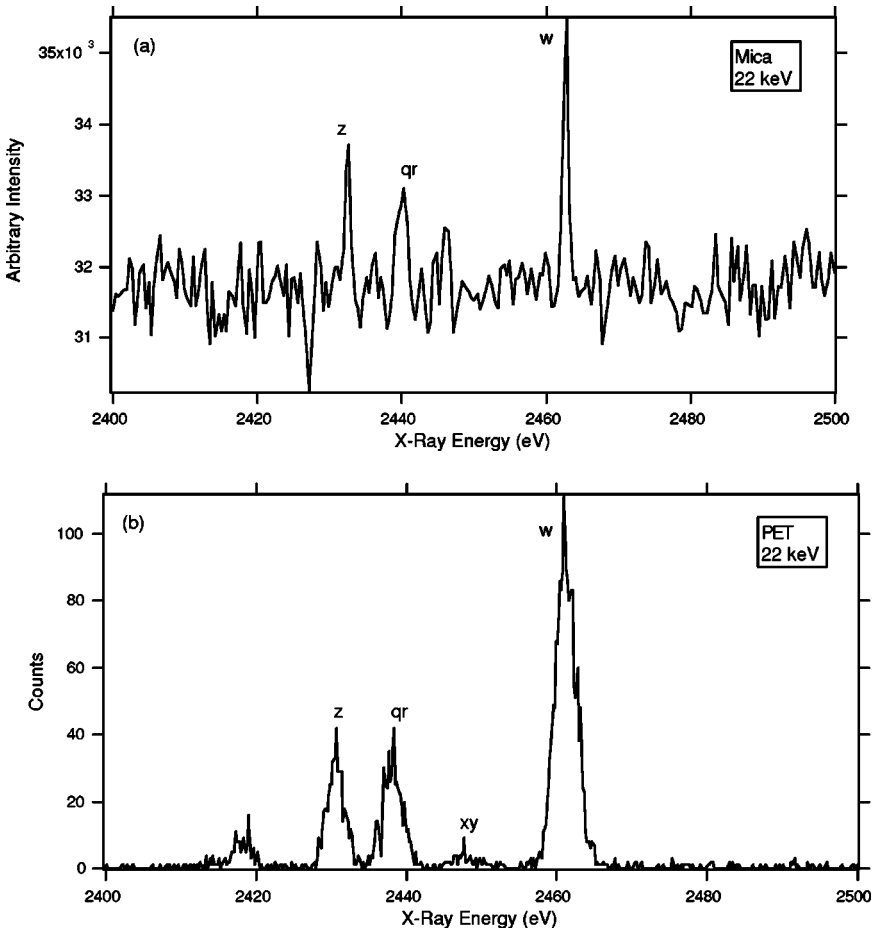

FIG. 3. Spectra obtained with (a) the spherically bent crystal spectrometer and (b) the flat crystal spectrometer (electron beam energy: 22 keV).

$$I^{obs} = R_{\|} I_{\|} + R_{\perp} I_{\perp}, \tag{1}$$

where $R_{\|}$ and $R_{\perp}$ represent the integrated crystal reflectivities for x-ray emission polarized parallel and perpendicular to the plane of dispersion, respectively. $I_{\|}$ and $I_{\perp}$ denote the intensity of the emitted radiation with an electric field vector parallel and perpendicular to the electron beam direction, respectively. The integrated crystal reflectivities are commonly written as the ratio $R \equiv R_{\perp}/R_{\|}$. This ratio varies as a function of the Bragg angle and is tabulated by Henke *et al.* [23] for a variety of crystals including PET (002) and Mica (002) crystals used for this experiment. The polarization of emission lines observed at an angle of $\vartheta = 90°$ from the electron beam is defined as

$$P = \frac{I_{\|} - I_{\perp}}{I_{\|} + I_{\perp}}. \tag{2}$$

As stated earlier, the two crystal spectrometers act as polarimeters. The FCS is oriented in a geometry that preferably reflects $I_{\|}$, but I^{obs}_{PET} also contains contributions from $I_{\perp}$, since the PET crystal used in the FCS was set at a Bragg angle of $\theta_B = 35.2°$, which corresponds to an integrating crystal reflectivity ratio of $R_{\mathrm{PET}} \sim 0.28$. The spherical crystal spectrometer was set at a Bragg angle close to 45° corresponding to a ratio of $R_{\mathrm{Mica}} \sim 0.04$. As a result, the spherical crystal spectrometer absorbs most of $I_{\|}$ while reflecting $I_{\perp}$. The measured intensities of the spherical crystal spectrometer in the following are approximated as

$$I^{obs}_{\mathrm{Mica}} = R_{\perp} I_{\perp}. \tag{3}$$

When using the "two-crystal technique" to infer polarization of line emissions it is convenient to normalize the line intensity of interest to a line emission unaffected by polarization (or to a line emission where P is known either experimentally or theoretically). In our case, the observed line emission is normalized to the forbidden z line ($1s2s\ ^3S_1 \rightarrow 1s^2\ ^1S_0$) in heliumlike sulfur. The $1s2s\ ^3S_1 \rightarrow 1s^2\ ^1S_0$ transition is readily observed in the spectra measured with either spectrometer. Line z is intrinsically unpolarized, but can be slightly polarized due to cascades [13]. Applying this normalization, the intensity ratio of lines of interest can be written as

$$\left(\frac{I^w}{I^z}\right)_{\mathrm{Mica}} = \frac{I^w_{\perp}}{I^z_{\perp}} \tag{4}$$

for intensities observed with the spherically bent crystal

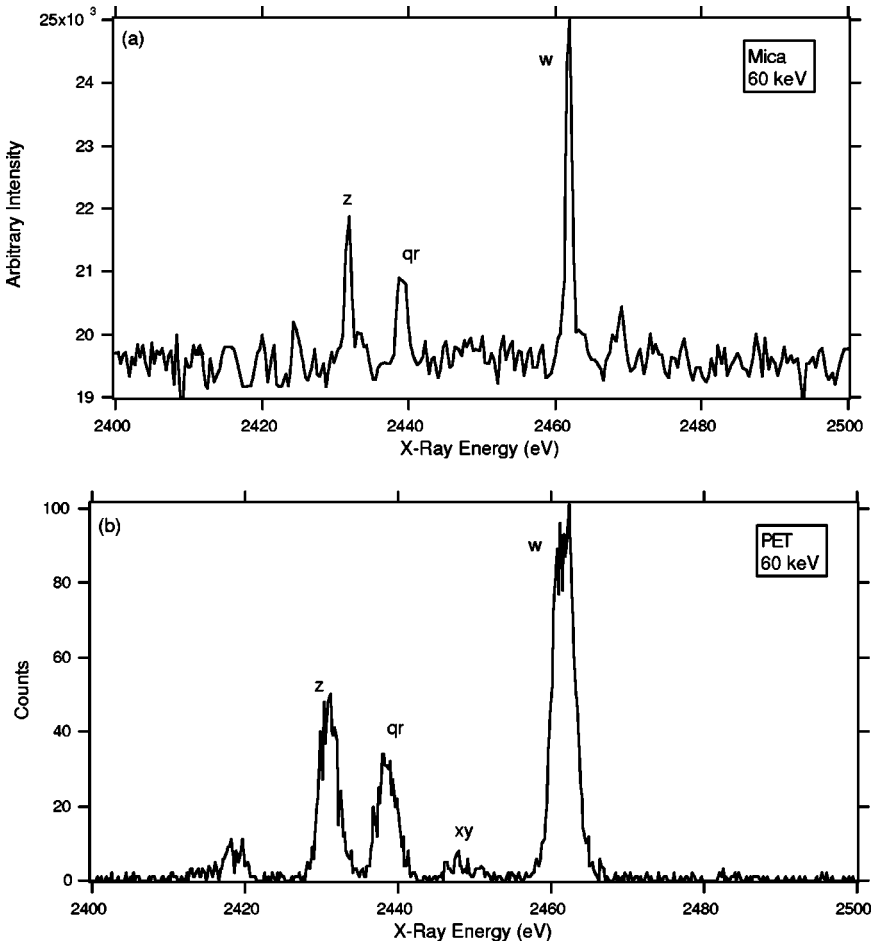

FIG. 4. Spectra obtained with (a) the spherically bent crystal spectrometer and (b) the flat crystal spectrometer (electron beam energy: 60 keV).

spectrometer. As for intensities observed with the FCS this ratio becomes

$$\left(\frac{I^w}{I^z}\right)_{\mathrm{PET}} = \frac{I_{\parallel}^w + R_{\mathrm{PET}} I_{\perp}^w}{I_{\parallel}^z + R_{\mathrm{PET}} I_{\parallel}^z}. \tag{5}$$

Combining Eqs. (2), (4), and (5) we derive an expression for the polarization of resonance line of He-like sulfur,

$$P_w = \frac{\left[\left(\frac{1+P_z}{1-P_z}\right) + R_{\mathrm{PET}}\right]\left(\frac{I^w}{I^z}\right)_{\mathrm{PET}} - \left(\frac{I^w}{I^z}\right)_{\mathrm{Mica}}(R_{\mathrm{PET}}+1)}{\left[\left(\frac{1+P_z}{1-P_z}\right) + R_{\mathrm{PET}}\right]\left(\frac{I^w}{I^z}\right)_{\mathrm{PET}} + \left(\frac{I^w}{I^z}\right)_{\mathrm{Mica}}(R_{\mathrm{PET}}-1)}. \tag{6}$$

The terms $(I^w/I^z)_{\mathrm{PET}}$ and $(I^w/I^z)_{\mathrm{Mica}}$ are obtain from Gaussian fits of the spectra (see Table I). Since the spectra shown in Figs. 2–5 were taken concurrently, the polarization of the blended resonance line of Li-like sulfur (P_{qr}) can be calculated from Eq. (6) by simply replacing I^w with I^{qr}. Where I^{qr} denotes the line intensity blend of Li-like sulfur resonance lines $1s2s2p\ ^2P_{3/2} \rightarrow 1s^2 2s\ ^2S_{1/2}$ and $1s2s2p\ ^2P_{1/2} \rightarrow 1s^2 2s\ ^2S_{1/2}$.

The slight polarization of line *z* due to cascades can be determined entirely by the branching ratios of the upper levels [13]. Using the flexible atomic code (FAC) [24], we calculated cascades contributions from $n \leqslant 3$ (cascades contributions from $n > 3$ are considered negligible). The predicted values of P_z are listed in Table I. As for the theoretical predictions of P_w and P_{qr}, we again use FAC as well as the distorted-wave (DW) computer code developed by Zhang *et al.* [25]. Since the polarization is due to the preferential population of the magnetic sublevels, both computer codes are used to calculate the magnetic sublevel cross sections of the resonance lines of interests:

$$P_w = \frac{\sigma_0 - \sigma_1}{\sigma_0 + \sigma_1}, \tag{7}$$

$$P_q = \frac{3\sigma_{1/2} - 3\sigma_{3/2}}{5\sigma_{1/2} + 3\sigma_{3/2}}. \tag{8}$$

In Eq. (7) σ_0 and σ_1 denote the cross sections for electron impact excitation from the ground state to the $m=0$ and 1 magnetic sublevels for He-like ion resonance transition, $1s2p\ ^1P_1 \rightarrow 1s^2\ ^1S_0$. Similarly, in Eq. (8) $\sigma_{1/2}$ and $\sigma_{3/2}$ denote the magnetic sublevel cross sections concerning Li-like ion resonance transition, $1s2s2p\ ^2P_{3/2} \rightarrow 1s^2 2s\ ^2S_{1/2}$. The polar-

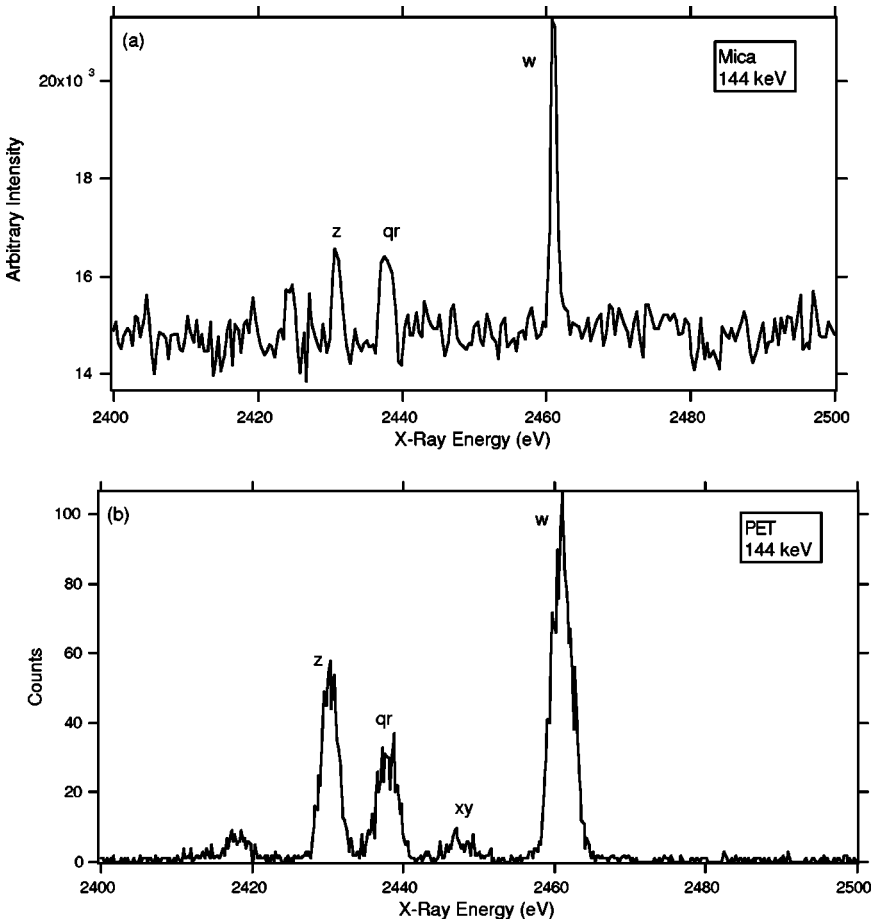

FIG. 5. Spectra obtained with (a) the spherically bent crystal spectrometer and (b) the flat crystal spectrometer (electron beam energy: 144 keV).

ization of the blend of the Li-like sulfur resonance lines can be written as

$$P_{rq} = \frac{\beta_r P_r \sigma_r + \beta_q P_q \sigma_q}{\beta_r \sigma_r + \beta_q \sigma_q}, \tag{9}$$

where σ_q and σ_r denote the total electron impact excitation cross sections for two transitions $1s2s2p\ ^2P_{3/2} \rightarrow 1s^2 2s\ ^2S_{1/2}$ and $1s2s2p\ ^2P_{1/2} \rightarrow 1s^2 2s\ ^2S_{1/2}$, respectively [since the latter's total angular momentum of its upper state is 1/2, $P_r = 0$ in Eq. (9)]. Also note that the branching ratios β_r and β_q in Eq. (9) are both approximately equal to 0.80 [24]. While the distorted-wave method uses a fully relativistic approach to calculate magnetic sublevel cross sections due to electron impact, FAC uses a quasirelativistic approximation which

TABLE I. Intensities observed with the FCS and the spherically bent crystal spectrometer for the resonance lines of S^{13+}, S^{14+}, and the forbidden *z* line of S^{14+}.

Beam energy (keV)	Counts[a]						
	I^w_{PET}	I^w_{Mica} [b]	I^{qr}_{PET}	I^{qr}_{Mica} [b]	I^z_{PET}	I^z_{Mica} [b]	P_z^{Theory} [c]
3	364	52	117	139	77	−0.18	
6	1480	44	282	19	322	32	−0.15
12	1326	41	387	17	384	21	−0.07
22	1478	76	428	34	440	42	∼0
30	1681	91	423	16	452	33	∼0
60	1540	115	430	34	614	47	−0.04
100	1104	131	359	40	427	51	−0.08
144	1425	147	440	46	657	43	−0.10

[a]Intensities were obtained from the Gaussian fit of the lines.
[b]Converted counts from the CCD detector [120 "CCD counts" ≈ 1 real count (Ref. [26])].
[c]FAC predictions of the polarization of line *z* due to cascades ($n \leqslant 3$).

TABLE II. Polarization measurements for the resonance line of S^{13+} and S^{14+} compared to theoretical predictions obtained with FAC and the relativistic distorted-wave (DW) computer code.

Beam energy (keV)	P_w^{measured}	P_w^{DW}	P_w^{FAC}	$P_{qr}^{\text{measureda}}$	P_{qr}^{DW}	P_{qr}^{FAC}
3	$0.55^{+0.15}_{-0.15}$	0.61	0.61		0.20	0.19
6	$0.51^{+0.09}_{-0.09}$	0.49	0.49	$0.10^{+0.13}_{-0.13}$	0.18	0.16
12	$0.30^{+0.10}_{-0.10}$	0.30	0.29	$0.05^{+0.12}_{-0.12}$	0.11	0.09
22	$0.32^{+0.09}_{-0.09}$	0.14	0.10	$0.11^{+0.11}_{-0.11}$	0.05	0.02
30	$0.16^{+0.08}_{-0.08}$	0.06	−0.01		0.02	−0.01
60	$-0.03^{+0.07}_{-0.07}$	−0.11	−0.21	$-0.06^{+0.10}_{-0.10}$	−0.03	−0.07
100	$-0.06^{+0.09}_{-0.09}$	−0.23	−0.32	$-0.02^{+0.11}_{-0.11}$	−0.07	−0.10
144	$-0.37^{+0.07}_{-0.07}$	−0.30	−0.37	$-0.42^{+0.09}_{-0.09}$	−0.10	−0.12

[a]Due to high noise level of the spherical crystal spectrometer, we are not able to infer P_{qr} at electron impact energies 3 and 30 keV.

gives adequate results for low to mid Z elements [24].

IV. DISCUSSION AND CONCLUSION

The results are summarized in Table II and compared to theoretical predictions. Unlike the results reported in Ref. [18], the measured polarization agrees well with our predictions made with the Flexible Atomic Code and the relativistic distorted-wave code. The measured values and predictions are also shown in Figs. 6 and 7. The error bars in both figures represent the quadrature sum of the statistical error and the high noise level of the CCD detector used with the compact spherical crystal spectrometer. Also shown in Fig. 6 are the nonrelativistic predictions of Itikawa *et al.* [10]. These early predictions are limited from near threshold of the resonance line of He-like sulfur (~2.5 keV) up to 12 keV, but nevertheless agree well with both the predictions of FAC and DW for this limited energy region. The measured polarization for the blended resonance lines of Li-like sulfur as a function of electron impact energy ($1s2s2p\ ^2P_{3/2} \rightarrow 1s^2 2s\ ^2S_{1/2}$ and $1s2s2p\ ^2P_{1/2} \rightarrow 1s^2 2s\ ^2S_{1/2}$) compared to the predictions of FAC and DW show fair agreement as well.

ACKNOWLEDGMENTS

We graciously acknowledge the support by the Lawrence Livermore National Laboratory Research Collaborations

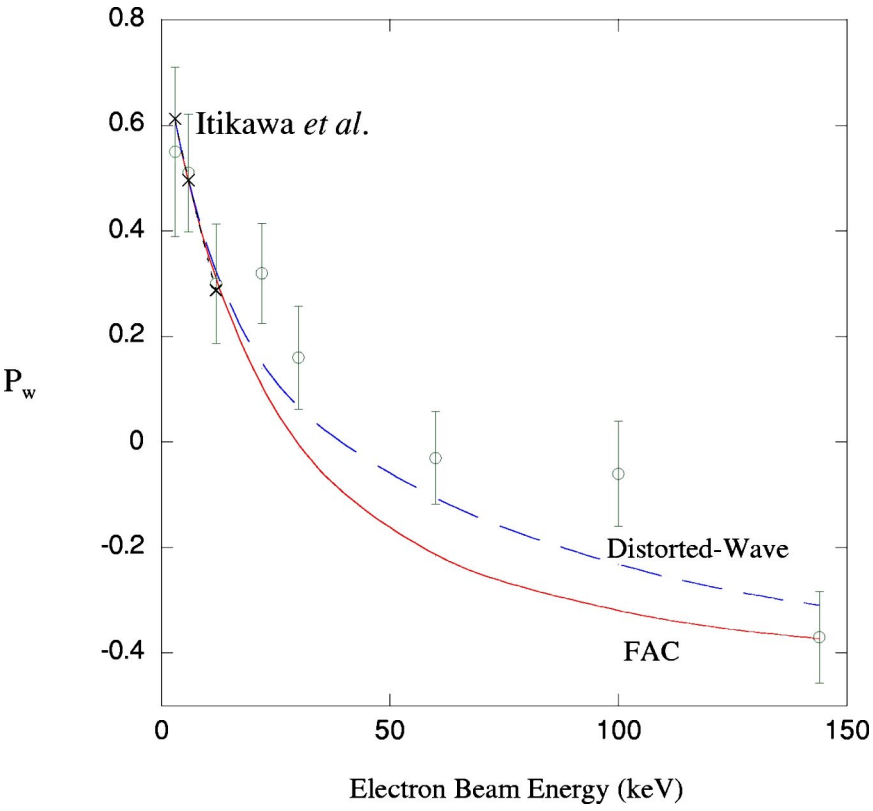

FIG. 6. Measured polarization of the resonance line of helium-like sulfur compared to the predictions of FAC and distorted-wave calculations. The nonrelativistic predictions of Itikawa from 3 to 12 keV are also shown.

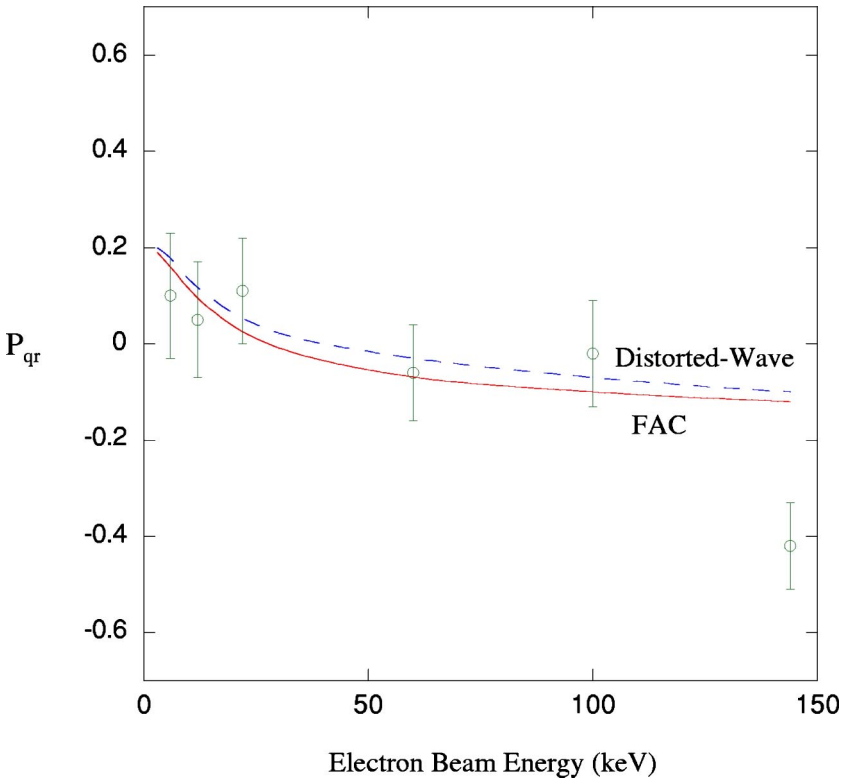

FIG. 7. Measured polarization of the resonance line of lithium-like sulfur compared to the predictions of FAC and distorted-wave calculations.

Programs for HBCU. This work was performed under the auspices of the U.S. Department of Energy by Lawrence Livermore National Laboratory under Contract No. W-7405-ENG-48 and by Morehouse College under Contract No. DE-FG02-98ER14877. We also acknowledge the NATO Collaborative Linkage Grant No. PST.CLG.97889.

[1] M.K. Inal and J. Dubau, J. Phys. B **20**, 4221 (1987).
[2] E. Haug, Sol. Phys. **71**, 77 (1981).
[3] J.C. Kieffer, J.P. Matte, M. Chaker, Y. Beaudoin, C.Y. Chien, S. Coe, G. Mourou, J. Dubau, and M.K. Inal, Phys. Rev. E **48**, 4648 (1993).
[4] R. Beier, C. Bachmann, and R. Burhenn, J. Phys. D **14**, 643 (1981).
[5] A.S. Shlyaptseva, S.B. Hansen, V.L. Kantsyrev, B.S. Bauer, D.A. Fedin, N. Ouart, S.A. Kazantsev, A.G. Petrashen, and U.I. Safronova, Rev. Sci. Instrum. **72**, 1241 (2001).
[6] A.S. Shlyaptseva, V.L. Kantsyrev, N. Ouart, D. Fedin, S. Hamasha, and S. Hansen, Proc. SPIE **5196**, 16 (2003).
[7] P. Beiersdorfer and M. Slater, Phys. Rev. E **64**, 066408 (2001).
[8] A.S. Shlyaptseva and R.C. Mancini, J. Quant. Spectrosc. Radiat. Transf. **58**, 917 (1997).
[9] K.J. Reed and M.H. Chen, Phys. Rev. A **48**, 3644 (1993).
[10] Y. Itikawa, R. Srivastava, and K. Sakimoto, Phys. Rev. A **44**, 7195 (1991).
[11] H.L. Zhang, D.H. Sampson, and R.E.H. Clark, Phys. Rev. A **41**, 198 (1990).
[12] J.R. Henderson, P. Beiersdorfer, C.L. Bennett, S. Chantrenne, D.A. Knapp, R.E. Marrs, M.B. Schneider, K.L. Wong, G.A. Doschek, J.F. Seely, C.M. Brown, R.E. LaVilla, J. Dubau, and M.A. Levine, Phys. Rev. Lett. **65**, 705 (1990).
[13] P. Beiersdorfer, D.A. Vogel, K.J. Reed, V. Decaux, J.H. Scofield, K. Widmann, G. Hölzer, E. Förster, O. Wehrhan, D.W. Savin, and L. Schweikhard, Phys. Rev. A **53**, 3974 (1996).
[14] P. Beiersdorfer, J. Crespo López-Urrutia, V. Decaux, K. Widmann, and P. Neil, Rev. Sci. Instrum. **68**, 1073 (1997).
[15] A.S. Shlyaptseva, R.C. Mancini, P. Neil, and P. Beiersdorfer, Rev. Sci. Instrum. **68**, 1095 (1997).
[16] E. Takács, E.S. Meyer, J.D. Gillaspy, J.R. Roberts, C.T. Chantler, L.T. Hudson, R.D. Deslattes, C.M. Brown, J.M. Laming, J. Dubau, and M.K. Inal, Phys. Rev. A **54**, 1342 (1996).
[17] P. Beiersdorfer, G. Brown, S. Utter, P. Neil, K.J. Reed, A.J. Smith, and R.S. Thoe, Phys. Rev. A **60**, 4156 (1999).
[18] N. Nakamura, D. Kato, N. Miura, T. Nakahara, and S. Ohtani, Phys. Rev. A **63**, 024501 (2001).
[19] D.A. Knapp, R.E. Marrs, S.R. Elliott, E.W. Magee, and R. Zasadzinski, Nucl. Instrum. Methods Phys. Res. A **334**, 305 (1993).
[20] G.V. Brown, P. Beiersdorfer, and K. Widmann, Rev. Sci. Instrum. **70**, 280 (1999).
[21] N. Nakamura, E. Nojikawa, H. Shiraishi, F.J. Currell, S. Ohtani, A. Ya. Faenov, and T.A. Pikuz, Rev. Sci. Instrum. **70**, 1658 (1999).
[22] B.K.F. Young, A.L. Osterheld, D.F. Price, R. Shepherd, R.E. Stewart, A. Ya. Faenov, A.I. Magunov, T.A. Pikuz, I. Yu. Sko-

belev, F. Flora, S. Bollanti, P. Di Lazzaro, T. Letardi, A. Grilli, L. Palladino, A. Reale, A. Scafati, and L. Reale, Rev. Sci. Instrum. **69**, 4049 (1998).
[23] B.L. Henke, E.M. Gullikson, and J.C. Davis, At. Data Nucl. Data Tables **54**, 181 (1993).
[24] M.F. Gu (private communication, Flexible Atomic Code).
[25] H.L. Zhang, D.H. Sampson, and R.E.H. Clark, Phys. Rev. A **41**, 198 (1990).
[26] J. Dunn, B.K.F. Young, A.D. Conder, and R.E. Stewart, Proc. SPIE **2654**, 119 (1996).